CORA Cork Open Research Archive
Cartlann Taighde Oscailte Chorcaí

Title	Recovery of steady rotational wave profiles from pressure measurements at the bed
Authors	Clamond , Didier;Labarbe, Joris , Joris;Henry , David
Publication date	2023-04-24
Original Citation	Clamond, D., Labarbe, J. and Henry, D. (2023) 'Recovery of steady rotational wave profiles from pressure measurements at the bed', Journal of Fluid Mechanics, 961, R2 (11pp). https://doi.org/10.1017/jfm.2023.271
Type of publication	Article (peer-reviewed)
Link to publisher's version	10.1017/jfm.2023.271
Rights	© 2023, Cambridge University Press. This material is free to view and download for personal use only. Not for re-distribution, re-sale or use in derivative works. - https://creativecommons.org/licenses/by-nc-nd/4.0/
Download date	2026-11-03 12:25:59
Item downloaded from	https://hdl.handle.net/10468/14332



UCC
University College Cork, Ireland
Coláiste na hOllscoile Corcaigh

Recovery of steady rotational wave profiles from pressure measurements at the bed

Didier Clamond[1]†, Joris Labarbe[1] and David Henry[2]

[1]Université Côte d'Azur, CNRS UMR 7351, Laboratoire J. A. Dieudonneé, Parc Valrose, 06108 Nice cedex 2, France

[2]School of Mathematical Sciences, University College Cork, Cork, Ireland

(Received xx; revised xx; accepted xx)

We derive equations relating the pressure at a flat seabed and the free-surface profile for steady gravity waves with constant vorticity. The resulting set of nonlinear equations enables the recovery of the free surface from pressure measurements at the bed. Furthermore, the flow vorticity is determined solely from the bottom pressure as part of the recovery method. This approach is applicable even in the presence of stagnation points and its efficiency is illustrated via numerical examples.

1. Introduction

In this paper, we present a formulation of the rotational water wave problem which enables the recovery of nonlinear surface gravity wave profiles from pressure measurements at the seabed, for steady flows with constant vorticity. The determination of the wave profile is achieved by numerically solving a set of nonlinear equations, with our inverse recovery procedure having the significant side-benefit of also determining the vorticity ω directly from bottom pressure measurements. The presence of vorticity greatly complicates the mathematical problem, and the recovery of fully nonlinear rotational water wave profiles from pressure measurements has hitherto proven unattainable (although explicit surface-profile recovery formulae for linear, and weakly nonlinear, rotational water waves were derived by Henry & Thomas (2018) for arbitrary vorticity distributions).

The reconstruction of water wave surface profiles from bottom pressure measurements is a theoretically challenging issue with important applications in marine engineering. Measuring the surface of water waves directly is difficult and costly, particularly in the ocean, so a commonly employed alternative is to calculate the free-surface profile of water waves using measurements from submerged pressure transducers. To do so requires the construction of either a suitable pressure-transfer function (for linear waves), or a surface reconstruction procedure (for nonlinear waves), the determination of which corresponds to a difficult mathematical problem.

Until quite recently, most surface reconstruction formulae were applicable only to the restricted setting of linear water waves, and even then solely for irrotational flows. First approaches towards surface reconstruction formulae for nonlinear irrotational waves appeared in (Constantin 2012; Oliveras *et al.* 2012), however these formulae are quite involved. Exact tractable relations were derived in (Clamond 2013; Clamond & Constantin 2013) which permit a straightforward numerical procedure for deriving the free surface from the bottom pressure. A significant advantage of these approaches is that they work directly with nonlinear waves in the physical plane, allowing recovery of nonlinear wave-profiles up to, and including, Stokes wave of greatest height (Clamond & Henry

† Email address for correspondence: didier.clamond@univ-cotedazur.fr

2020). The robustness of this nonlinear wave surface reconstruction approach is further illustrated in this paper by expanding it to encompass flows with constant vorticity.

Incorporating vorticity in the water wave problem is vital for capturing fundamental physical processes relating to wave-current interactions (Thomas & Klopman 1997), however it significantly complicates all theoretical considerations (Constantin 2011). We note that while it was rigorously proven by Henry (2013) that the profile-recovery problem is well-posed for nonlinear *solitary* waves with arbitrary (real analytic) vorticity distributions, it remains an open question whether the inverse recovery problem is well-posed for *periodic* waves. Even in the simplified setting of constant vorticity, the water wave problem exhibits features not encountered in the irrotational case. In particular, we note such flows may contain stagnation points (and critical layers) in the fluid interior, and waves which possess overhanging profiles. The possibility of overhanging waves was first observed numerically (Da Silva & Peregrine 1988; Okamoto & Shoji 2001) and their possible existence was recently rigorously proven (Constantin & Varvaruca 2011; Constantin *et al.* 2016). We note that the surface recovery approach introduced in this paper is applicable to flows containing stagnation points, however we must exclude overhanging profiles *a priori*. It is assumed throughout that the surface profile is a graph (overhanging waves cannot occur for 'downstream' waves, c.f. Constantin *et al.* (2021)).

2. Preliminaries

In the frame of reference moving with a travelling wave of permanent shape, the flow beneath the wave reduces to a steady motion with respect to the moving coordinate system. Thus, the wave phase velocity c is constant in any Galilean frame of reference. Let (x, y) be a Cartesian coordinate system moving with the wave, x being the horizontal coordinate and y the upward vertical coordinate. We define accordingly the fluid domain as $\Omega = \{(x, y) : x \in \mathbb{R}, -d \leqslant y \leqslant \eta(x)\}$, where $y = -d$ and $y = \eta(x)$ correspond, respectively, to the solid bottom and the free-surface (both impermeable). In addition, $(u(x, y), v(x, y))$ denotes the velocity field in the moving frame. We assume the wave is $L = (2\pi/k)$-periodic (with $k \to 0$ for solitary waves) in the x-direction, and we denote by $y = 0$ the mean water level. The latter equation expresses the fact that $\langle\eta\rangle = 0$, where $\langle\cdot\rangle$ is the Eulerian average operator over one period, that is,

$$\langle\eta\rangle \stackrel{\text{def}}{=} \frac{k}{2\pi}\int_{-\pi/k}^{\pi/k} \eta(x)\mathrm{d}x = 0. \tag{2.1}$$

The flow is governed by the balance between the restoring gravity force and the inertia of the system. With constant density $\rho > 0$, the equation of mass conservation and Euler equations (defined in Ω) are, respectively,

$$\partial_x u + \partial_y v = 0, \quad u\partial_x u + v\partial_y u = -\partial_x P/\rho, \quad u\partial_x v + v\partial_y v = -\partial_y P/\rho - g, \quad (2.2a, b, c)$$

where $P(x, y)$ denotes the pressure. As a general notation, subscripts 'b' denote all quantities written at the bed $y = -d$ whereas subscripts 's' denote all quantities written at the free surface $y = \eta(x)$. The effect of surface tension being neglected, on the free surface we must have the dynamic boundary condition

$$P_{\mathrm{s}} = P_{\mathrm{atm}}, \tag{2.3}$$

where P_{atm} is the (constant) atmospheric pressure. The free surface and the rigid bed are impermeable interfaces, giving the kinematic boundary conditions (with $\eta_x \stackrel{\text{def}}{=} \mathrm{d}\eta(x)/\mathrm{d}x$)

$$v_{\rm s} = u_{\rm s}\eta_x, \qquad v_{\rm b} = 0, \tag{2.4a, b}$$

respectively, while the rotational character of the flow is ensured by requiring

$$\partial_x v - \partial_y u \stackrel{\rm def}{=} \omega \quad (= \text{constant}). \tag{2.5}$$

Equations (2.2)–(2.5) are the governing equations for rotational (of constant vorticity ω) travelling water waves in a frame of reference moving with the wave.

For incompressible flows where (2.2a) holds we can define a streamfunction ψ such that $u = \partial_y\psi$ and $v = -\partial_x\psi$. As the flow is steady and the free-surface is impermeable, it follows that the free-surface is a streamline, that is, the streamfunction is constant $\psi = \psi_{\rm s}$ at the free-surface (similarly, the streamfunction is constant $\psi = \psi_{\rm b}$ at the bed).

Equations (2.2) can be integrated to

$$2p + 2gy + u^2 + v^2 = B_{\rm s} - 2\omega(\psi - \psi_{\rm s}), \tag{2.6}$$

for some constant $B_{\rm s}$, where $p(x,y) \stackrel{\rm def}{=} [P(x,y) - P_{\rm atm}]/\rho$ is a normalised relative pressure. Equation (2.6) is a Bernoulli equation, and we note that the Bernoulli integral $B(\psi) \stackrel{\rm def}{=} B_{\rm s} - 2\omega(\psi - \psi_{\rm s})$ is constant for an irrotational motion (i.e., when $\omega = 0$).

3. Definition of the parameters

From the definition (2.1) of the mean water level and by averaging expression (2.6) written at the free surface, we obtain a definition for the constant $B_{\rm s}$ in the form

$$B_{\rm s} = \left\langle u_{\rm s}^2 + v_{\rm s}^2 \right\rangle. \tag{3.1}$$

As the frame of reference moving with the wave is Galilean, there is no mean acceleration. For steady waves with constant vorticity, the zero-mean horizontal acceleration condition is perforce satisfied, but the condition for zero mean vertical acceleration yields

$$\begin{aligned} 0 &= \left\langle \int_{-d}^{\eta} \left[u\frac{\partial v}{\partial x} + v\frac{\partial v}{\partial y} \right] {\rm d}y \right\rangle = \left\langle \int_{-d}^{\eta} \frac{\partial}{\partial y} \left[\frac{u^2+v^2}{2} + \omega\psi \right] {\rm d}y \right\rangle \\ &= \tfrac{1}{2}\left\langle u_{\rm s}^2 + v_{\rm s}^2 \right\rangle - \tfrac{1}{2}\left\langle u_{\rm b}^2 \right\rangle + \omega\left(\psi_{\rm s} - \psi_{\rm b}\right). \end{aligned} \tag{3.2}$$

This furnishes at once an alternative relation for the Bernoulli constant

$$B_{\rm s} = \left\langle u_{\rm b}^2 \right\rangle + 2\omega\left(\psi_{\rm b} - \psi_{\rm s}\right), \tag{3.3}$$

and, since $p_{\rm s} = 0$, relation (3.2) implies the average pressure at the bottom is

$$\langle p_{\rm b} \rangle = -\left\langle \int_{-d}^{\eta} \frac{\partial p}{\partial y} {\rm d}y \right\rangle = \left\langle \int_{-d}^{\eta} \left[u\frac{\partial v}{\partial x} + v\frac{\partial v}{\partial y} + g \right] {\rm d}y \right\rangle = gd. \tag{3.4}$$

Relation (3.4) provides a mechanism for determining the mean water depth d from bottom pressure measurements. For later convenience, define the alternative Bernoulli constant

$$B_{\rm b} \stackrel{\rm def}{=} B_{\rm s} - 2\omega\left(\psi_{\rm b} - \psi_{\rm s}\right) = \left\langle u_{\rm b}^2 \right\rangle, \tag{3.5}$$

where, as expected, both Bernoulli constants $B_{\rm b}$ and $B_{\rm s}$ coincide for irrotational flows. The vorticity ω being constant, exploiting the free surface impermeability gives

$$\begin{aligned} \omega d &= \left\langle \int_{-d}^{\eta} \left[\frac{\partial v}{\partial x} - \frac{\partial u}{\partial y} \right] {\rm d}y \right\rangle = -\left\langle \eta_x v_{\rm s} \right\rangle - \left\langle u_{\rm s} \right\rangle + \left\langle u_{\rm b} \right\rangle \\ &= \left\langle u_{\rm b} \right\rangle - \left\langle \left(1 + \eta_x^2\right) u_{\rm s} \right\rangle. \end{aligned} \tag{3.6}$$

Expression (3.6) provides a means of determining the vorticity ω in terms of u_b, u_s, d and η. In the same vein, a relation not involving velocity evaluation along the flat bed is given by

$$\frac{\omega}{2}\left\langle h^2\right\rangle = \left\langle \int_{-d}^{\eta}\left[\frac{\partial v}{\partial x}-\frac{\partial u}{\partial y}\right](y+d)\mathrm{d}y\right\rangle = -\left\langle h\eta_x v_\mathrm{s}\right\rangle - \left\langle hu_\mathrm{s}\right\rangle + \psi_\mathrm{s} - \psi_\mathrm{b}$$
$$= \psi_\mathrm{s} - \psi_\mathrm{b} - \left\langle \left(1+\eta_x^2\right) hu_\mathrm{s}\right\rangle, \tag{3.7}$$

where $h(x) \overset{\text{def}}{=} \eta(x) + d$ is the total water depth. Together with (3.5), relation (3.7) can be expressed

$$B_\mathrm{s} = B_\mathrm{b} - \omega^2\left\langle h^2\right\rangle - 2\omega\left\langle \left(1+\eta_x^2\right) hu_\mathrm{s}\right\rangle. \tag{3.8}$$

As for irrotational motions, Stokes' first and second definitions of the phase celerities (Clamond 2017; Kishida & Sobey 1988) can be applied, resulting in the expressions

$$c_1 \overset{\text{def}}{=} -\left\langle u_\mathrm{b}\right\rangle = -\omega d - \left\langle \left(1+\eta_x^2\right) u_\mathrm{s}\right\rangle, \tag{3.9}$$

$$c_2 \overset{\text{def}}{=} -\left\langle \frac{1}{d}\int_{-d}^{\eta} u\mathrm{d}y\right\rangle = \frac{\psi_\mathrm{b}-\psi_\mathrm{s}}{d} = -\frac{\omega d}{2} - \frac{\omega\left\langle\eta^2\right\rangle}{2d} - \frac{\left\langle \left(1+\eta_x^2\right) hu_\mathrm{s}\right\rangle}{d}. \tag{3.10}$$

Here c_1 and c_2 are the wave speeds observed in frames of reference without mean horizontal velocity at the bed, and without mean flow, respectively. In the irrotational case ($\omega = 0$), it can be shown (Clamond & Dutykh 2018) that $c_2 \to c_1$ and $B_\mathrm{b} = B_\mathrm{s} \to c_1^2$ as $d \to \infty$ or as $k \to 0$, but $c_2 \approx c_1$ in the linear wave regime. For constant vorticity $\omega \neq 0$, matters are more complex, even at the linear level: $c_2 \approx c_1 - \omega d/2 \not\approx c_1$, while $c_1 \approx c_0^{\pm}$ where the linear phase speed (Brink-Kjær 1976; Kishida & Sobey 1988)

$$c_0^{\pm} = -\omega d + \tfrac{1}{2}k^{-1}\omega\tanh(kd) \pm \tfrac{1}{2}k^{-1}\sqrt{\omega^2\tanh(kd)^2 + 4gk\tanh(kd)}, \tag{3.11}$$

solves a linear dispersion relation with symmetry property $c_0^{\pm}(-\omega) = -c_0^{\mp}(\omega)$. Hence, without loss of generality in subsequent considerations, we assume that $c_1 > 0$ (that is, the wave propagates toward the increasing x-direction in the frame of reference without mean velocity at the seabed) and allow the vorticity to take either sign.

4. Holomorphic functions

When $\omega = 0$ the flow is irrotational and one can use the powerful theory of holomorphic functions (Clamond 2013; Clamond & Constantin 2013; Clamond & Henry 2020). In the case where $\omega \neq 0$ one can still use this technique following Helmholtz representation (Aris 1962). Thus, introducing U, V and Ψ (functions of both x and y) as

$$U \overset{\text{def}}{=} u + \omega(y+d), \qquad V \overset{\text{def}}{=} v, \qquad \Psi \overset{\text{def}}{=} \psi + \tfrac{1}{2}\omega(y+d)^2, \tag{4.1a,b,c}$$

from which, using (2.5), straightforward calculations show that $U = \partial_y\Psi$, $V = -\partial_x\Psi$ and $\partial_x V = \partial_y U$, implying that the velocity field (U, V) is curl-free. At the bed $y = -d$, we have

$$U_\mathrm{b} = u_\mathrm{b}, \qquad V_\mathrm{b} = v_\mathrm{b} = 0, \qquad \Psi_\mathrm{b} = \psi_\mathrm{b}, \tag{4.2a,b,c}$$

while at the free surface $y = \eta(x)$

$$U_\mathrm{s} = u_\mathrm{s} + \omega h, \qquad V_\mathrm{s} = v_\mathrm{s}, \qquad \Psi_\mathrm{s} = \psi_\mathrm{s} + \tfrac{1}{2}\omega h^2. \tag{4.3a,b,c}$$

Note that Ψ_s is not uniform (unlike ψ_s) while Ψ_b is a constant. Thus, introducing a velocity potential Φ such that $U = \partial_x\Phi$ and $V = \partial_y\Phi$, the complex potential and velocity

are defined as

$$F(z) \stackrel{\text{def}}{=} \Phi + \mathrm{i}\Psi, \qquad W(z) \stackrel{\text{def}}{=} U - \mathrm{i}V = \mathrm{d}F/\mathrm{d}z, \tag{4.4a, b}$$

where $z \stackrel{\text{def}}{=} x + \mathrm{i}y$ is a complex coordinate in Ω. With these new dependent variables, the Bernoulli equation (2.6) evaluated at the free surface becomes

$$U_\mathrm{s}^2 + V_\mathrm{s}^2 + 2\,(g\eta - \omega h U_\mathrm{s}) + (\omega h)^2 = B_\mathrm{s}, \tag{4.5}$$

while at the bed it yields

$$2\,(p_\mathrm{b} - gd) + U_\mathrm{b}^2 = B_\mathrm{s} - 2\omega\,(\psi_\mathrm{b} - \psi_\mathrm{s}) = \langle U_\mathrm{b}^2 \rangle = B_\mathrm{b}. \tag{4.6}$$

Note that equations (4.5) and (4.6) can be rewritten, respectively,

$$U_\mathrm{s} = \omega h - \sqrt{(B_\mathrm{s} - 2g\eta)/(1+\eta_x^2)}, \qquad U_\mathrm{b} = -\sqrt{B_\mathrm{b} - 2\,(p_\mathrm{b} - gd)}, \tag{4.7a, b}$$

the minus sign in front of the radicals being consequence of the choice $c_1 > 0$. Since $V_\mathrm{b} = 0$, the complex velocity can then be expressed as

$$W(z) = -\sqrt{B_\mathrm{b} - 2p_\mathrm{b}(z + \mathrm{i}d) + 2gd}, \tag{4.8}$$

a relation which suggests the introduction of a complex pressure. Following Clamond & Constantin (2013), we introduce a 'complex pressure' function $\mathfrak{P}$ defined as

$$\mathfrak{P}(z) \stackrel{\text{def}}{=} gd + \omega\,(\psi_\mathrm{s} - \psi_\mathrm{b}) - \tfrac{1}{2}\left(W^2 - B_\mathrm{s}\right), \tag{4.9}$$

which is holomorphic in the fluid domain Ω. Note that the expression in (4.9) is purely real when restricted to the flat bed, with $\mathfrak{P}_\mathrm{b} = p_\mathrm{b}$ on $y = -d$. Accordingly, p_b determines $\mathfrak{P}$ uniquely within the entire fluid domain Ω, and so $\mathfrak{P}(z) = p_\mathrm{b}(z + \mathrm{i}d)$. We note that since p is not a harmonic function in the fluid domain (Constantin 2011), it can coincide with the real part of $\mathfrak{P}$ only at $y = -d$.

Similarly, as for irrotational waves in (Clamond 2013, 2018), it is useful to introduce the holomorphic function $\mathfrak{Q}$

$$\mathfrak{Q}(z) \stackrel{\text{def}}{=} \int_{z_0}^{z} [\mathfrak{P}(z') - gd]\,\mathrm{d}z' = \frac{1}{2}\int_{z_0}^{z} \left[B_\mathrm{b} - W(z')^2\right]\mathrm{d}z', \tag{4.10}$$

where $z_0 \in \Omega$ is an arbitrary constant.

5. Equations for the surface recovery

Integrating (4.10) along the free surface path, with the origin located at the crest (i.e. $z_0 = \mathrm{i}a$, $a \stackrel{\text{def}}{=} \eta(0)$ being the wave amplitude), one gets

$$\mathfrak{Q}_\mathrm{s}(x) = \int_0^x [\mathfrak{P}_\mathrm{s}(x') - gd]\,(1 + \mathrm{i}\eta_x')\,\mathrm{d}x', \tag{5.1}$$

where $\mathfrak{P}_\mathrm{s}(x) = gd + (B_\mathrm{b} - U_\mathrm{s}^2 + V_\mathrm{s}^2)/2 + \mathrm{i}U_\mathrm{s}V_\mathrm{s}$. With (2.4a), (4.3a,b), (4.7a) and splitting real and imaginary parts, (5.1) yields after some algebra

$$\begin{aligned}\mathfrak{Q}_\mathrm{s}(x) = \int_0^x &\left[\mathrm{Re}\left\{\mathfrak{P}_\mathrm{s}(x')\right\} - gd - \mathrm{Im}\left\{\mathfrak{P}_\mathrm{s}(x')\right\}\eta_x'\right]\mathrm{d}x' \\ &+ \mathrm{i}(\eta - a)\left[\hat{B} - \tfrac{1}{2}(g + \omega^2 d)(\eta + a) - \tfrac{1}{6}\omega^2\left(\eta^2 + a\eta + a^2\right)\right],\end{aligned} \tag{5.2}$$

where $\hat{B} \stackrel{\text{def}}{=} (B_\mathrm{s} + B_\mathrm{b} - \omega^2 d^2)/2$ is an expression involving Bernoulli constants at the surface and the bottom. The imaginary part of (5.2) provides an implicit relation for the

surface elevation expressed in terms of the holomorphic function $\mathfrak{Q}_\mathrm{s}$

$$\mathrm{Im}\{\mathfrak{Q}_\mathrm{s}\} = (\eta - a)\left[\hat{B} - \tfrac{1}{2}(g+\omega^2 d)(\eta + a) - \tfrac{1}{6}\omega^2\left(\eta^2 + a\eta + a^2\right)\right]. \tag{5.3}$$

From the differentiation of (5.1) and (5.3), one gets the differential equation

$$\frac{\mathrm{d}\eta}{\mathrm{d}x} = \frac{\mathrm{Im}\{\mathfrak{P}_\mathrm{s}\}}{\hat{B} - (g+\omega^2 d)\eta - \frac{1}{2}\omega^2\eta^2 - \mathrm{Re}\{\mathfrak{P}_\mathrm{s}\} + gd}. \tag{5.4}$$

In the special case of irrotational motion ($\omega = 0$), the differential equation derived in Clamond & Constantin (2013) is recovered. Evaluating (5.3) at the trough ($x = -\pi/k$), bearing in mind relation (3.8), one obtains an expression for $\hat{B}$ as

$$\begin{aligned}\hat{B} &= B_\mathrm{s} + \tfrac{1}{2}\omega^2\left\langle\eta^2\right\rangle - \omega\left\langle h\sqrt{(B_\mathrm{s} - 2g\eta)(1+\eta_x^2)}\right\rangle,\\ &= \tfrac{1}{2}(g+\omega^2 d)(a-b) + \tfrac{1}{6}\omega^2(a^2 - ab + b^2) - (a+b)^{-1}\,\mathrm{Im}\{\mathfrak{Q}_\mathrm{s}(-\pi/k)\},\end{aligned} \tag{5.5}$$

where $b \overset{\text{def}}{=} -\eta(-\pi/k)$ denotes the trough height (thus $H \overset{\text{def}}{=} a+b$ is the total wave height).

We now have algebraic expressions for the recovery of η and $\hat{B}$, as functions of the remaining unknown parameters a, b and ω. Three relations are then needed to close our set of equations. These relations are obtained considering $\mathfrak{P}_\mathrm{s} = gd + \omega\,(\psi_\mathrm{s} - \psi_\mathrm{b}) - \frac{1}{2}\left(W_\mathrm{s}^2 - B_\mathrm{s}\right)$ at the crest, at the trough and at an intermediate point. Using the surface impermeability with the decomposition (4.1), the squared complex velocity reduces to

$$\begin{aligned}W_\mathrm{s}^2 &\overset{\text{def}}{=} (U_\mathrm{s} - \mathrm{i}V_\mathrm{s})^2 = \omega^2 h^2 + 2\omega h u_\mathrm{s}\,(1 - \mathrm{i}\eta_x) + u_\mathrm{s}^2\,(1 - \mathrm{i}\eta_x)^2,\\ &= \omega^2 h^2 + \left[(B_\mathrm{s} - 2g\eta)/(1 + \mathrm{i}\eta_x) - 2\omega h\sqrt{(B_\mathrm{s} - 2g\eta)/(1+\eta_x^2)}\right](1 - \mathrm{i}\eta_x).\end{aligned} \tag{5.6}$$

Following Clamond & Constantin (2013), we substitute (5.6) in the definition of $\mathfrak{P}_\mathrm{s}$ at the crest and the trough — together with (3.8) and (3.10) — to get the two relations

$$\mathfrak{P}_\mathrm{s}(0) = gh_c + \omega^2\frac{\langle h^2\rangle - h_c^2}{2} - \omega\left[\left\langle h\sqrt{(B_\mathrm{s} - 2g\eta)(1+\eta_x^2)}\right\rangle - h_c\sqrt{B_\mathrm{s} - 2ga}\right], \tag{5.7}$$

$$\mathfrak{P}_\mathrm{s}\left(-\frac{\pi}{k}\right) = gh_t + \omega^2\frac{\langle h^2\rangle - h_t^2}{2} - \omega\left[\left\langle h\sqrt{(B_\mathrm{s} - 2g\eta)(1+\eta_x^2)}\right\rangle - h_t\sqrt{B_\mathrm{s} + 2gb}\right], \tag{5.8}$$

where $h_t \overset{\text{def}}{=} d - b$ and $h_c \overset{\text{def}}{=} d + a$ are local depths under, respectively, the trough and the crest. As expected, both expressions reduce in the irrotational limit to the formulae derived in Clamond (2013). With (5.7) and (5.8) we have two relations that close the problem if ω is known. However, in practice ω is generally unknown *a priori*, so another independent relation must be introduced.

A last relation is obtained considering the complex pressure $\mathfrak{P}_\mathrm{s}$ at an abscissa x_0 strictly between crest and trough. This point is chosen at a coordinate of median bottom pressure measurement such that $p_\mathrm{b}(x_0) = (\max p_\mathrm{b} - \min p_\mathrm{b})/2$ to ensure a large distance from the crest and the trough. x_0 being thus chosen, $\mathrm{Im}\{\mathfrak{Q}_\mathrm{s}(x_0)\}$, $\mathrm{Re}\{\mathfrak{P}_\mathrm{s}(x_0)\}$ and $\mathrm{Im}\{\mathfrak{P}_\mathrm{s}(x_0)\}$ (together with (5.6) applied at x_0) provide three relations for $\eta(x_0)$, $\eta_x(x_0)$ and ω (relations not written *in extenso* here, for brevity).

6. Reconstruction procedure

From measurements of the bottom pressure p_b, the free surface reconstruction procedure takes the following form. The first step is to choose a suitable basis of functions, generally a Fourier polynomial or elliptic functions (Clamond 2013; Clamond & Constantin 2013). The best choice is the one providing the best fit among data with a

minimum of eigenfunctions. Here, we consider only Fourier polynomials for simplicity, but the procedure is identical for any basis of functions expressible in the complex plane. Thus, the wavenumber k and the coefficients $\mathfrak{p}_n$ of the Nth order Fourier polynomials $p_\mathrm{b} \approx \sum_{n=-N}^{N} \mathfrak{p}_n \mathrm{e}^{\mathrm{i}nkx}$, can be determined by least-square minimisation (Clamond & Barthélémy 1995). From (3.4), we know that $\mathfrak{p}_0 = gd$ and, since the acceleration due to gravity g is known, this relation gives an expression for the mean water depth d. Thus, after this first step, parameters g, d, k and $\mathfrak{p}_n$ are known explicitly and the bottom pressure can be extended everywhere in the bulk of the fluid.

From the analytic approximation of p_b, the holomorphic pressure $\mathfrak{P}$ is, by definition,

$$\mathfrak{P}(z) \approx \sum_{n=-N}^{N} \mathfrak{p}_n \mathrm{e}^{\mathrm{i}nk(z+\mathrm{i}d)} = \sum_{n=-N}^{N} \mathfrak{p}_n \mathrm{e}^{-nkd} \mathrm{e}^{\mathrm{i}nkz}, \tag{6.1}$$

so one obtains at once

$$\mathfrak{Q}_\mathrm{s}(x) = \int_0^x [\mathfrak{P}_\mathrm{s}(x') - gd]\,\mathrm{d}x' \approx \sum_{|n|>0}^{N} \frac{\mathrm{i}\mathfrak{p}_n}{nk} \frac{\mathrm{e}^{-nka} - \mathrm{e}^{\mathrm{i}nk(x+\mathrm{i}\eta)}}{\mathrm{e}^{-nkd}}. \tag{6.2}$$

After this second step, $\mathfrak{P}_\mathrm{s}$ and $\mathfrak{Q}_\mathrm{s}$ are known explicitly as functions of η. The wave surface profile η is then determined solving the algebraic (i.e. not differential, nor integral) equation (5.3) which, in general, can only be achieved numerically. This results in η being obtained as a function of the parameters a, b, ω and B_s. These parameters are then determined solving the nonlinear equations (5.5), (5.7), (5.8) and the ones at x_0.

The numerical procedure consists in solving simultaneously the nonlinear set of equations (5.3), (5.5), (5.7), (5.8) (and the ones at x_0) to recover the surface wave profile and related parameters. To this end, we use an iterative root-finding algorithm (the built-in function fsolve in MATLAB) supplemented with initial values given by the linear theory (Kishida & Sobey 1988). When needed, η_x is computed directly from its explicit expression (5.4).

7. Example

In order to validate our procedure, we computed exact rotational waves with an accurate numerical algorithm similar to that of Da Silva & Peregrine (1988). We then obtained bottom pressures that are considered the 'measured' ones from which the free surface and vorticity are recovered. Throughout the procedure, we monitor the convergence of our iterative algorithm using a tolerance of 10^{-12}. When converged, the numerical solution is compared with the exact surface wave profile η^ex and vorticity ω^ex.

For waves of relatively small amplitudes, as well as small ω, we witness a rapid convergence of the recovery procedure described above. The numerical errors of the recovered surface and vorticity are, respectively, $\epsilon_\eta = \|\eta - \eta^\mathrm{ex}\|_\infty < 10^{-8}$ and $\epsilon_\omega = |\omega - \omega^\mathrm{ex}| < 10^{-6}$. This excellent agreement is reached with as few as $N = 5$ harmonics when considering the pressure Fourier expansion. However, for steady rotational waves with a steeper profile (thus departing from linear theory), the procedure naturally requires a larger number of harmonics.

Here, we illustrate our surface wave recovery procedure with numerical examples depicted in Figures 1 and 2 for a domain of size $L/d = 2\pi$ (rather deep water for which surface recovery is *a priori* difficult). For our first example, we examine a steep wave with negative vorticity $\omega\sqrt{d/g} = -1.7$. Although the steep wave in figure 1c would appear to be quite challenging to compute, we still recover the correct surface profile using $N = 30$

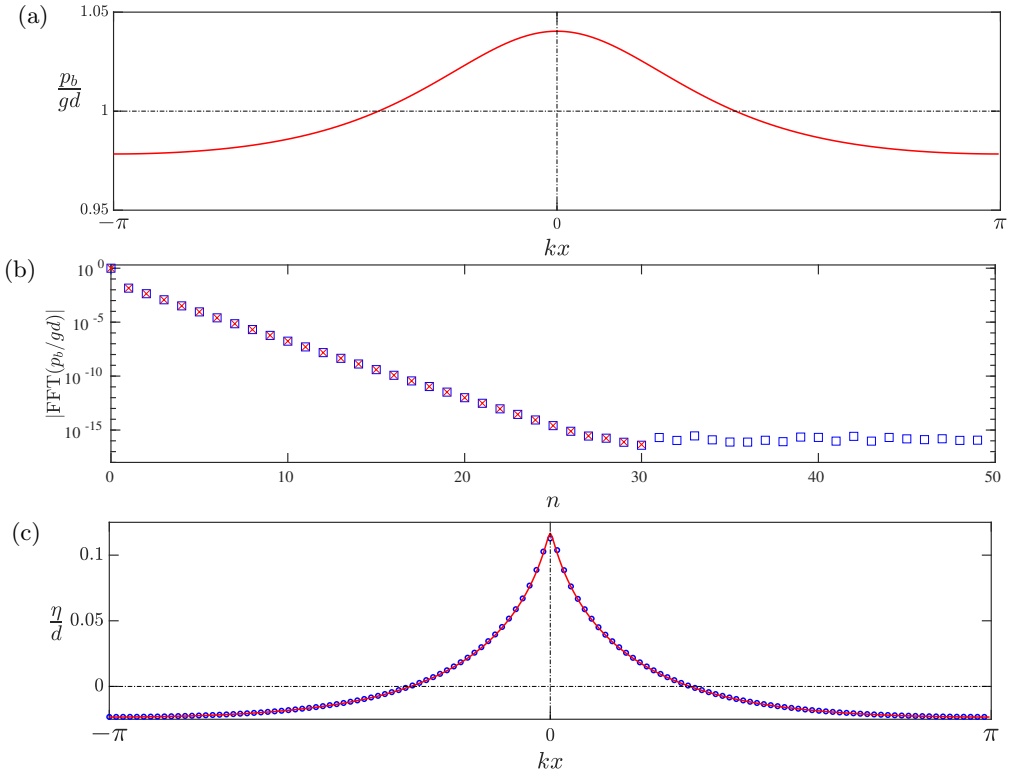


Figure 1: Example of surface recovery for $\omega\sqrt{d/g} = -1.7$, $H/d = 0.14$ and $L/d = 2\pi$: (a) pressure at the bottom; (b) Fourier spectrum extracted from bottom pressure (blue squares) and fitted harmonics used for the reconstruction (red crosses); (c) recovered wave profile (red line) versus exact surface profile (blue circles).

harmonics in our Fourier expansion (c.f. panel 1b), with the recovered solutions showing an excellent agreement with the exact data ($\epsilon_\eta \approx 10^{-4}$ and $\epsilon_\omega \approx 10^{-4}$).

For the second case of interest (Figure 2), we take the positive vorticity $\omega\sqrt{d/g} = 3$. This value is greater than that predicated by linear wave theory for the existence of critical layers. Indeed, linear waves with $c_0 > 0$ never allow for stagnation points when $\omega < 0$, while they contain stagnation points for $\omega > 0$ iff $\tanh(kd)/kd \leqslant \omega^2 d/(g + \omega^2 d)$ (Constantin & Varvaruca 2011; Da Silva & Peregrine 1988). This example is of special interest because it involves three stagnation points per wavelength: two at the bottom (about half way between crests and troughs) and one within the fluid (under the crests), c.f. Figure 14a of Da Silva & Peregrine (1988). The surface recovery still works relatively well in this case; taking $N = 20$ Fourier modes, errors are $\epsilon_\eta \approx 10^{-3}$ and $\epsilon_\omega \approx 10^{-4}$ (see Figure 2).

We observe from panel 1a that the bottom pressure distribution for our choice of wave configuration displays a monotonic increase between trough and crest, which is not matched by that illustrated in panel 2a. This is not an artefact solely of the difference in signs of the vorticities, but rather also their magnitudes — an examination of explicit linear solutions for water waves with constant vorticity (Brink-Kjær 1976) illustrates the richness in behaviour of the pressure fluctuations even for small amplitude waves, both with regard to its monotonicity properties, and the location of its extrema. For nonlinear waves, the precise qualitative behaviour of the bottom pressure fluctuations due to wave

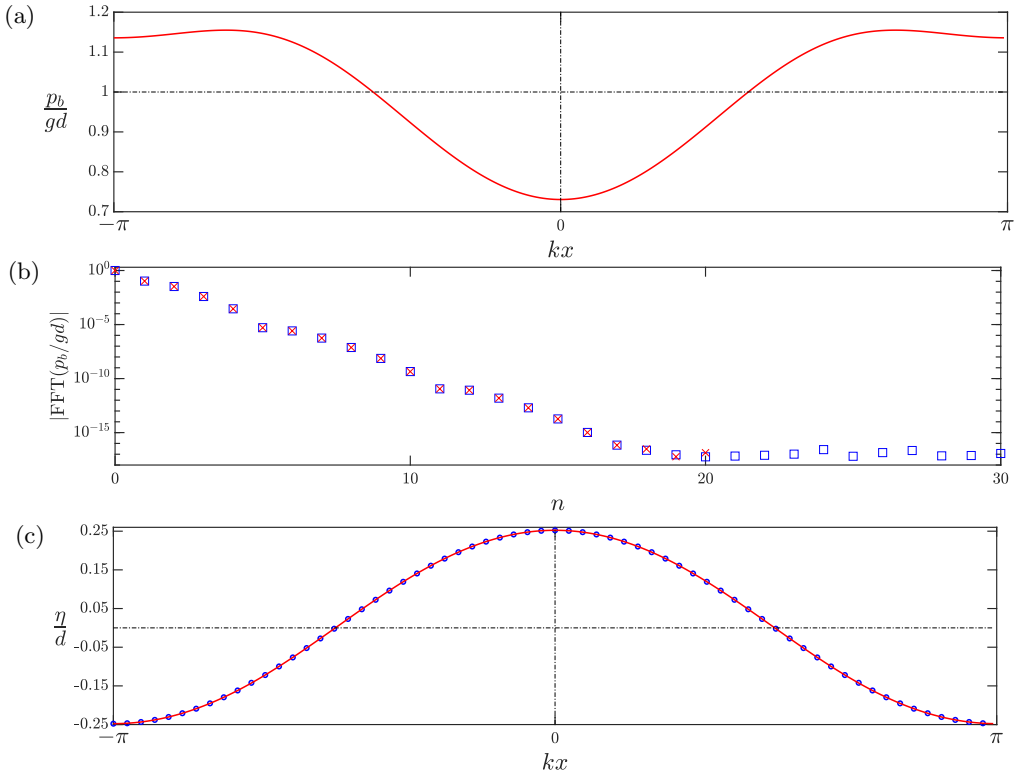


Figure 2: Same as Figure 1 for the case $\omega\sqrt{d/g} = 3$, $H/d = 0.5$ and $L/d = 2\pi$.

motion (and the location of its extrema) was only recently rigorously established for irrotational periodic waves in (Constantin 2016), and there are presently no similarly rigorous mathematical results for nonlinear waves with constant vorticity. It is clear from panels 1a and 2a that considerable insight into this matter can be gained from a numerical approach.

8. Discussion

In this paper, we have presented a procedure for recovering fully nonlinear wave surface profiles from bottom pressure measurements for flows with constant vorticity. The theoretical basis for this procedure involves a reformulation in terms of holomorphic functions $\mathfrak{P}$ and $\mathfrak{Q}$, respectively introduced in (Clamond & Constantin 2013) and (Clamond 2013), followed by a numerical implementation scheme. We have demonstrated the efficiency of this approach for different flow regimes, including one which presents stagnation points in the fluid body (an archetypical feature of waves with constant vorticity). For future work, it would be interesting to expand our approach to incorporate variable vorticity. Additionally, the question remains open as to whether our approach can be adapted to recover waves which exhibit overhanging profiles.

Funding. Joris Labarbe has been supported by the French government, through the UCA$^{\text{JEDI}}$ *Investments in the Future* project managed by the National Research Agency (ANR) with the reference number ANR-15-IDEX-01. David Henry acknowledges the

support of the Science Foundation Ireland (SFI) under the grant SFI 21/FFP-A/9150.

Declaration of interests. The authors report no conflict of interest.

REFERENCES

Aris, R. 1962 *Vectors, tensors and basic equations of fluid mechanics*. Dover.

Brink-Kjær, O. 1976 Gravity waves on a current: The influence of vorticity, a sloping bed, and dissipation. In *Institute of Hydrodynamics and Hydraulic Engineering*, *(ISVA)* 12, pp. 1–137. Technical University of Denmark.

Clamond, D. 2013 New exact relations for easy recovery of steady wave profiles from bottom pressure measurements. *J. Fluid Mech.* **726**, 547–558.

Clamond, D. 2017 Remarks on Bernoulli constants, gauge conditions and phase velocities in the context of water waves. *App. Math. Lett.* **74**, 114–120.

Clamond, D. 2018 New exact relations for steady irrotational two-dimensional gravity and capillary surface waves. *Phil. Trans. R. Soc. A* **376** (2111), 20170220.

Clamond, D. & Barthélémy, E. 1995 Experimental determination of the phase shift in the Stokes wave – solitary wave interaction. *C. R. Ac. Sci. Paris IIb* **320** (6), 277–280.

Clamond, D. & Constantin, A. 2013 Recovery of steady periodic wave profiles from pressure measurements at the bed. *J. Fluid Mech.* **714**, 463–475.

Clamond, D. & Dutykh, D. 2018 Accurate fast computation of steady two-dimensional surface gravity waves in arbitrary depth. *J. Fluid Mech.* **844**, 491–518.

Clamond, D. & Henry, D. 2020 Extreme water-wave profile recovery from pressure measurements at the seabed. *J. Fluid Mech.* **903**, R3, 12.

Constantin, A. 2011 *Nonlinear water waves with applications to wave-current interactions and tsunamis*, *CBMS-NSF Regional Conference Series in Applied Mathematics*, vol. 81. SIAM, Philadelphia, PA.

Constantin, A. 2012 On the recovery of solitary wave profiles from pressure measurements. *J. Fluid Mech.* **699**, 376–384.

Constantin, A. 2016 Extrema of the dynamic pressure in an irrotational regular wave train. *Physics of Fluids* **28** (11), 113604.

Constantin, A., Strauss, W. & Varvaruca, E. 2016 Global bifurcation of steady gravity water waves with critical layers. *Acta Math.* **217** (2), 195–262.

Constantin, A., Strauss, W. & Varvaruca, E. 2021 Large-amplitude steady downstream water waves. *Comm. Math. Phys.* **387** (1), 237–266.

Constantin, A. & Varvaruca, E. 2011 Steady periodic water waves with constant vorticity: regularity and local bifurcation. *Arch. Ration. Mech. Anal.* **199** (1), 33–67.

Da Silva, A. T. & Peregrine, D. H. 1988 Steep, steady surface waves on water of finite depth with constant vorticity. *J. Fluid Mech.* **195**, 281–302.

Henry, D. 2013 On the pressure transfer function for solitary water waves with vorticity. *Math. Ann.* **357** (1), 23–30.

Henry, D. & Thomas, G. P. 2018 Prediction of the free-surface elevation for rotational water waves using the recovery of pressure at the bed. *Philos. Trans. Roy. Soc. A* **376** (2111), 20170102, 21.

Kishida, N. & Sobey, J. 1988 Stokes theory for waves on linear shear current. *J. Engin. Mech.* **114** (8), 1317–1334.

Okamoto, H. & Shoji, M. 2001 *The mathematical theory of permanent progressive water-waves*, *Advanced Series in Nonlinear Dynamics*, vol. 20. World Scientific Publishing Co., Inc., River Edge, NJ.

Oliveras, K. L., Vasan, V., Deconinck, B. & Henderson, D. 2012 Recovering the water-wave profile from pressure measurements. *SIAM J. Appl. Math.* **72** (3), 897–918.

Thomas, G.P. & Klopman, G. 1997 Wave-current interactions in the nearshore region. In *Gravity waves in water of finite depth* (ed. J. N. Hunt), *Advances in Fluid Mechanics* , pp. 255–319. Computational Mechanics Publications.